

Highlights

Reducing RES Droughts through the integration of wind and Solar PV

Boris Morin, Aina Maimó Far, Damian Flynn, Conor Sweeney

- RES droughts are analysed using 45 years of hourly wind and solar PV generation data
- RES droughts from C3S-Energy and ERA5-Atlite datasets are compared
- Adding solar PV to a wind-dominated system reduces RES drought frequency and duration
- Validated RES datasets are crucial to accurately identify RES drought extremes

Reducing RES Droughts through the integration of wind and Solar PV

Boris Morin^{a,*}, Aina Maimó Far^a, Damian Flynn^b, Conor Sweeney^a

*^aSchool of Mathematics and Statistics, University College Dublin, Belfield, Dublin
4, Dublin, D04 V1W8, Ireland*

*^bSchool of Electrical and Electronic Engineering, University College Dublin, Belfield,
Dublin 4, Dublin, D04 V1W8, Ireland*

*Corresponding author

Email addresses: `boris.morin@ucdconnect.ie` (Boris Morin),
`aina.maimofar@ucd.ie` (Aina Maimó Far), `damian.flynn@ucd.ie` (Damian Flynn),
`conor.sweeney@ucd.ie` (Conor Sweeney)

Abstract

Increasing the share of electricity produced from renewable energy sources (RES), combined with RES dependence on weather, poses a critical challenge for energy systems. This study investigates the importance of the balance between wind and solar photovoltaic (PV) capacity on periods of low renewable generation, known as RES droughts. Three different RES models are used to estimate the capacity factors for different scenarios of installed capacities for wind and solar PV power. The skill of the RES models is quantified by comparing capacity factor time series to observed hourly data and by assessing their representation of observed RES droughts. The RES models are used to generate a 45-year hourly time series of RES capacity factor, enabling analysis of the frequency, duration and return periods of RES droughts at a climatological scale. Results show the importance of using an accurate, validated RES model for RES drought risk assessment. The addition of solar PV capacity to a wind-dominated system results in a significant reduction in the frequency and duration of RES droughts, while also reducing extremes and seasonal drought patterns. These findings underscore the importance of diversification in RES capacity to enhance energy security and resilience.

Keywords: RES Drought, Wind Power, Solar PV Power, Renewable Energy Sources, Return Periods

1. Introduction

The EU aims to generate at least 69% of its electricity from renewable energy sources (RES) by 2030, up from 41% in 2022 [1]. While this transition is essential for reducing greenhouse gas emissions, it also highlights the challenge of managing the variability of weather-dependent energy sources such as wind and solar photovoltaic (PV) power. This challenge is amplified by the increasing electrification of energy sectors, which places greater demand on the power system and makes it more sensitive to meteorological conditions, both in historical [2] and future climates [3]. Periods of low renewable generation, known as *Dunkelflaute* or RES droughts, pose significant risks to system adequacy and energy security, emphasising the need for a resilient energy system to meet both growing electricity demand and decarbonisation targets.

RES drought events do not have a fixed definition, with various approaches present in the literature. One common method defines a RES drought as a period during which the average capacity factor (CF) remains below a fixed threshold for a specified duration. For example, Kaspar et al. [4] used this method to investigate the shortfall risks of low wind and solar PV generation in Europe, with a focus on Germany, testing multiple CF thresholds and durations. Similarly, Mockert et al. [5] examined the link between weather regimes and RES droughts in Germany using a 48-hour rolling window under a threshold to define RES droughts. Similar fixed-threshold approaches have also been applied using CF series reconstructed through machine learning in regions such as Japan [6] and Hungary [7].

Alternative methods adjust the CF threshold dynamically over the year to account for seasonal variations in renewable production. Raynaud et al. [8] defined droughts as sequences of days with energy production below a threshold that varies seasonally, a methodology later adapted for India [9]. Building on this, Kapica et al. [10] compared the likelihood of increased RES droughts in Europe under different climate models. Other studies have defined droughts based on deviations from daily mean production: Rinaldi et al. [11] applied these in the U.S. Western Interconnection to quantify the benefits of long-term storage, while Brown et al. [12] examined weekly timescales to explore meteorological influences on the most severe drought events. Another method defines energy drought indices based on metrics commonly used in hydro-meteorology to characterise RES droughts [13]. This approach identifies periods of unusually low generation relative to historical production levels, using the lowest production percentiles. Bracken et al. [14] used this approach to analyse RES droughts at different time scales in the U.S. [14], and Lei et al. [15] used it to quantify droughts in wind-PV-hydro systems in China.

In addition to examining periods of low renewable electricity generation, several studies also explore the periods when the imbalance between renewable generation and electricity demand (residual load) is high. Raynaud et al. [8] defined both energy production and energy supply droughts, and showed the difference in their patterns in a hypothetical fully renewable system composed of wind, PV and run-of-the-river hydropower. Similarly, Allen and Otero [13] also defined a standardised index based on meteorological droughts to address residual load, whose correlation to the energy production index is mostly negative (as expected, although quite low anticorrelations and even small positive correlations appear for some European countries). This

index was also applied to the U.S. by Bracken et al [14], revealing a consistent increase in the drought magnitude when load is considered, despite showing differing results across regions.

In this paper, the focus is exclusively on renewable electricity generation, which allows us to maintain physical models that do not consider the behavioural influence of demand, whose role will be addressed in the discussion. A fixed threshold approach is used to define RES droughts, which facilitates consistent inter-comparison between scenarios with different installed wind and solar PV capacities. The case study used in this paper is Ireland, a region with a strong reliance on wind power and ambitious targets for solar PV power expansion. This provides valuable insights into the potential benefits of diversifying the renewable energy mix on RES droughts in the context of realistic scenarios.

RES droughts are identified using onshore wind and solar PV CF time series. In this study, three different datasets are used and compared, all of which are driven by the ERA5 reanalysis [16]. Two of the datasets are part of C3S Energy (C3S-E), an energy-based operational dataset produced by the EU Copernicus Climate Change Service [17]. One of the C3S-E datasets provides CF time series aggregated at the national scale, while the other provides the CF time series at each grid point, at the ERA5 resolution of 0.25° . The third dataset was generated using the Atlite model [18], which converts the ERA5 atmospheric data to a generation time series using specified wind turbine and PV panel models. Atlite is an open-source tool developed by PyPSA [18] and has been used for estimating wind and solar PV generation in order to study RES droughts [5].

Generic datasets for wind and solar PV CF are often used for the quantification of RES droughts. Despite most of them undergoing a validation process, they are often not fully representative of all geographical locations, and even show strong differences between each other [19]. In this work, we quantify the skill of a generic model for Ireland (a region not commonly used for generic model validation), and explore the effect that using it has on RES droughts when compared to a specifically-designed model. This comparison is propagated through the whole analysis to fully see the effect of these differences in the context of a transition from a wind-only system to a more balanced mix that includes solar PV. In terms of the drought definition, the literature often uses daily averaged values, which limits the start and end times of events. We opt for a 24-hour rolling average, which avoids potential masking of day-long events due to their start time.

Therefore, the aim of this study is to answer three questions which could help on the decision making for the planning of reserve capacity in real case wind-dominated renewable energy system:

- Can generic datasets be used to quantify extreme events like RES droughts?
- What is the impact of modelling assumptions on the analysis of RES droughts?
- How does the integration of solar PV into a predominantly wind-based system alter the characteristics of RES droughts in a real-case setting?

The datasets used in this study are detailed in section 2, which describes their characteristics and relevance for evaluating RES droughts. Section 3 outlines the RES datasets used to simulate wind and solar PV generation and provides the methodology for defining and identifying RES drought events, including the thresholds and metrics applied. In section 4, the datasets are first verified against observed energy data to assess their accuracy, followed by an analysis of RES drought occurrences for two scenarios with different ratios of installed wind to solar PV capacities. Finally, section 5 offers a discussion of the results in the context of energy reliability and future planning, followed by the main conclusions and recommendations for further research.

2. Data

This study uses publicly available datasets to construct and validate the datasets for estimating the CF of wind and solar PV power. The primary data sources include: EirGrid and SONI, the transmission system operators (TSO) for the Republic of Ireland and Northern Ireland, respectively; the ERA5 reanalysis dataset; and the C3S-E datasets.

2.1. Wind and solar PV Capacity and Availability

EirGrid, the TSO for the Republic of Ireland, and SONI, the Northern Ireland TSO, provide detailed datasets on all wind and solar PV farms across the island of Ireland (Republic of Ireland and Northern Ireland) from 1990 to the present [20]. These datasets include information such as each farm's installed capacity, name, and connection date. To enhance the accuracy of this data, the longitude and latitude for each farm were manually determined

122 through online searches. For simplicity, this data will be referred to as orig-
 123 inating from EirGrid, as all-island data was directly obtained from EirGrid,
 124 and the combined regions of the Republic of Ireland and Northern Ireland
 125 will be referred to as Ireland throughout the remainder of this document.

126 The spreadsheet available from the EirGrid website contains two key vari-
 127 ables: generation and availability. Generation is the energy that a RES farm
 128 actually contributed to the grid, which may include limitations introduced
 129 by the TSO to maintain grid stability, such as constraints and curtailment.
 130 Availability represents the energy that would have been generated from a RES
 131 farm if no grid constraints had been applied, making it representative of the
 132 weather-related response. Generation and availability values are available
 133 from 2014 onward for wind power and from 2018 onward for solar PV power,
 134 although solar PV availability data only became present in the Republic of
 135 Ireland in 2023. This study focuses on availability for all analyses.

136 2.2. Atmospheric Variables

137 Atlite and C3S-E datasets are driven by the ERA5 reanalysis [16], pro-
 138 duced by the European Centre for Medium-Range Weather Forecasts (ECMWF).
 139 This global gridded dataset provides hourly atmospheric variables from 1940
 140 to the present at a horizontal resolution of 0.25° . It has proven to be the best
 141 choice for studying renewable energy in Ireland [21]. Table 1 lists the ERA5
 142 variables used by Atlite and C3S-Energy.

Table 1: ERA5 variables used to calculate wind and solar PV generation

ERA5 name	variable
100 metre zonal and meridional wind speed	u_{100}, v_{100}
2 metre temperature	$t2m$
Surface net solar radiation	ssr
Surface solar radiation downwards	$ssrd$
Top of atmosphere incident radiation	$tisr$
Total sky direct solar radiation at surface	$fdir$

143 2.3. C3S Energy

144 The EU Copernicus Climate Change Service developed the C3S-E renew-
 145 able energy dataset for Europe [17], using ERA5 atmospheric variables and
 146 weather-to-energy models. This dataset provides hourly CF for wind and

147 solar PV energy from 1979 to the present. The data are available on the
148 same grid as the ERA5 data, which has a horizontal resolution of 0.25° . The
149 time series are also available for download at two aggregated scales: regional
150 (NUTS 2) and national.

151 The wind CF in the C3S-E model is calculated using wind speeds at 100
152 metres (u_{100} , v_{100}) and a standard turbine model, the Vestas V136/3450,
153 with a fixed hub height of 100 meters. This choice reflects trends in wind
154 turbine installations and was guided by expert recommendations. Since real-
155 time data on the exact wind turbine fleet across Europe is difficult to obtain,
156 C3S-E assumes a homogeneous distribution of turbines across the ERA5 grid.
157 While this approach does not capture the precise capacity factors reported
158 by grid operators, it provides a well-correlated time series that effectively
159 represents the impact of climate variability on wind power generation. The
160 turbine power curves used in the model are sourced from publicly available
161 databases, ensuring consistency with industry standards. The solar PV CF
162 in the C3S-E model is calculated at the grid level and represents the aggre-
163 gated output of all solar PV systems within each pixel, rather than a single
164 installation. It is derived from meteorological data, including surface solar
165 radiation downwards ($ssrd$) and air temperature ($t2m$), using a reference
166 solar PV plant model. This model incorporates empirical calculations for
167 key system components such as optical losses, module efficiency, and invert-
168 ers. The final CF accounts for a mix of module orientations typical for each
169 location [22].

170 3. Methods

171 This study uses onshore wind and solar PV CF time series from three
172 datasets to analyse RES droughts across the island of Ireland. Data down-
173 loaded from C3S-E were used to obtain two datasets: one based on national-
174 level data (C3S-E N), and another on grid-level data (C3S-E G). The third
175 dataset was computed using the Atlite model (Atlite).

176 3.1. C3S-Energy National: C3S NAT

177 The C3S NAT dataset is created by combining different national and
178 regional data sources. The inputs used are the total installed capacity in
179 the Republic of Ireland and Northern Ireland, and the aggregated CF time
180 series provided by C3S-E at the two corresponding NUTS levels: Republic of
181 Ireland (NUTS0: IE) and Northern Ireland (NUTS2: UKN0). These values

are based on the assumption that RES generation occurs at every ERA5 grid point in Ireland. To get the C3S NAT CF for all of Ireland, a weighted average of the two obtained CF time series is performed, using the actual installed capacity as weights.

3.2. C3S-Energy Gridded: C3S GRID

The C3S GRID dataset combines information that contains the spatial variability over Ireland. The inputs used to create this dataset consist of the CF time series from C3S-E over the ERA5 grid, along with the location and characteristics of individual RES farms across Ireland, as explained in section 2.1. For each farm, the nearest grid point on the C3S-E dataset was identified, the generation from that farm was calculated using the retrieved CF from C3S-Energy, and it was added to a total generation. This total generation was divided by the total installed capacity to convert it back to CF. This is equivalent to performing a weighted average of the CF associated with each farm using the farm’s installed capacities as weights. The C3S GRID dataset contains the resulting CF time series, which accounts for the actual spatial distribution of wind and solar PV farms in Ireland.

3.3. Atlite: ATLITE

The ATLITE dataset is constructed by using the Atlite model to process weather variables into energy variables. This model allows for a tuning process where the models used to transform wind and solar PV can be adjusted to best represent the observed data up until this point for the relevant region (in this case, Ireland). The Atlite model takes as inputs the locations of RES farms and ERA5 weather variables: wind speed at 100 metres (u_{100} , v_{100}) for wind generation, and radiation variables (ssr , $ssrd$, $tisr$, and $fdir$) along with air temperature ($t2m$) for solar PV generation. These meteorological inputs are processed using the Atlite model to estimate CF time series for wind and solar PV, incorporating specific characteristics such as the wind turbine power curve and PV panel model selected for this specific case. The output of the Atlite model is a generation time series, which divided by the total capacity to transform it back into CF, which is what we call the ATLITE dataset. The flexibility in the usage of different power curves and PV panel models represents the key distinction between this dataset and the two C3S-derived ones. This study identifies the most appropriate wind turbine power curve to use from the 121 power curves at five different levels of smoothing made available by Renewables.ninja [23], and selects the PV panel model out

218 of the options available within the Atlite model. The selection of a specific
219 wind turbine and PV panel characteristics is further discussed and explained
220 in section 4.1.

221 3.4. *Energy Scenarios*

222 The output of those three datasets are one CF time series for both wind
223 and Solar PV. In addition to analysing wind and solar PV generation sep-
224 arately, a combined CF was computed for each dataset by averaging wind
225 and solar PV generation, weighted by their installed capacities at the end of
226 2023 (5.9 GW for wind power and 0.6 GW for solar PV power). This con-
227 figuration is referred to as the 91W-9PV scenario, reflecting the distribution
228 of 91% wind and 9% PV capacity. Given that solar PV capacity in Ireland
229 is low in 2023, and to explore how a more balanced distribution of wind and
230 solar PV capacities might impact RES droughts, this study also considered
231 a second scenario, referred to as 57W-43PV, where the installed solar PV ca-
232 pacity is assumed to increase to 8.6 GW, while wind capacity rises to 11.45
233 GW. These values are based on targets outlined in the roadmap published
234 by the 2024 Climate Action Plan [24]. This study does not include offshore
235 wind in the analysis. Recent reports suggest that even by 2030, Ireland
236 is unlikely to have any significant new offshore wind farms, with projected
237 offshore capacity expected to remain near zero using realistic scenarios [25].

238 New time series were generated for both the Atlite and C3S-E G solar
239 PV datasets, incorporating a revised distribution of installed capacity across
240 Ireland as specified in the roadmap. For wind power, the CF time series
241 remains unchanged, as significant shifts in the location of wind farms are not
242 expected. In total, twelve CF time series were analysed in this study, six for
243 individual wind and solar PV CF (three datasets for each source) in the 91W-
244 9PV scenario, and an additional six time series that include the combined
245 CF for 91W-9PV and 57W-43PV scenarios across the different datasets.

246 It is important to note that the specific capacity values used in this study
247 are illustrative and are not intended to reflect precise future realities. Instead,
248 they serve to explore the impact of transitioning from a wind-dominated sys-
249 tem (91W-9PV) to a more evenly distributed system (57W-43PV). This ap-
250 proach allows for a comparative analysis between the two scenarios, assessing
251 how the balance of RES capacity affects the occurrence of RES droughts.

252 For each dataset (Atlite, C3S-E G, and C3S-E N), four distinct scenarios
253 are examined, as summarised below:

- 254 • Wind Power - based on the actual capacity at the end of 2023
- 255 • Solar PV Power - based on the actual capacity at the end of 2023
- 256 • Combined RES / 91W-9PV - based on the actual capacity at the end
- 257 of 2023
- 258 • Combined RES / 57W-43PV - based on the capacity projected for 2030

259 3.5. RES Drought Definition

260 In this study, a RES drought event was defined as occurring when the
 261 24-hour moving average of CF remains below a fixed threshold of 0.1 for
 262 a period of longer than 24 hours. The choice of this threshold is somewhat
 263 arbitrary, but aligns with similar studies on low renewable energy production
 264 [4, 6, 7]. By using a 24-hour moving average, fewer but longer-lasting events
 265 were captured compared to using the raw CF time series, which can be more
 266 sensitive to short-term fluctuations. A fixed threshold approach was chosen
 267 in this study to enable consistent inter-comparison between datasets.

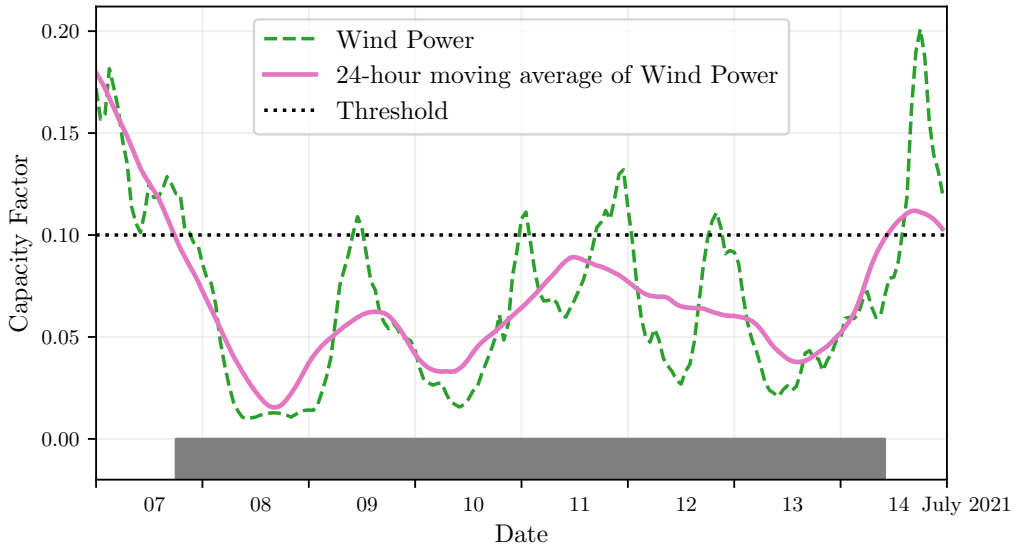


Figure 1: Wind time series of CF (green) and its 24-hour moving average (pink) from the 7th to the 15th of July 2021. The black dashed line indicates the CF threshold. The grey bar shows the period identified as a wind drought under our definition

268 The moving average approach smooths out short-term fluctuations, so
 269 that brief periods above the threshold do not interrupt an otherwise con-
 270 tinuous low-CF period (Fig. 1). This means that a single hour above the
 271 threshold does not "break" a drought event if it is surrounded by prolonged
 272 low-generation hours. As a result, fewer but longer-lasting drought events
 273 are identified, which may better reflect real-world conditions where energy
 274 supply constraints persist over extended periods.

275 4. Results

276 4.1. Verification

277 The accuracy of the datasets used in this study was verified, before con-
 278 tinuing to the analysis of RES droughts. For the verification process, time-
 279 varying values of installed capacity were used to account for changes in RES
 280 development over the verification period. This step allowed us to assess how
 281 well the datasets represent the production of renewable energy by comparing
 282 them against observed data.

283 4.1.1. Wind Energy

284 The C3S-E datasets use the Vestas V136/3450 wind turbine power curve,
 285 (Fig. 2a). The Atlite model allows the user to specify the power curve.
 286 We considered the 121 power curves available for download from Renew-
 287 ables.ninja [23]. For each power curve, Renewables.ninja also provides four
 288 associated smoothed power curves. The smoothing is done using a Gaussian
 289 filter with different standard deviations that depend on the wind speed. A
 290 separate wind CF time series for Ireland was generated for each of the wind
 291 turbine power curves and smoothing levels.

292 The performance of each CF time series is then assessed based on four skill
 293 scores: correlation coefficient (CC), root mean square error (RMSE), mean
 294 bias error (MBE), and the percentage of overlap. The percentage of overlap
 295 quantifies the similarity between the observed and modelled distributions. It
 296 is a positively oriented skill score, where 100% shows full agreement between
 297 the two distributions, and 0% indicates no overlap. The histograms of hourly
 298 CF values for the most recent decade (2014-2023) are used to calculate this
 299 skill score.

300 Based on these metrics, the most representative power curve for Ireland
 301 is the Enercon E112.4500 power curve with the $0.3w$ smoothing filter. The
 302 smoothing of the wind turbine power curve represents losses associated with

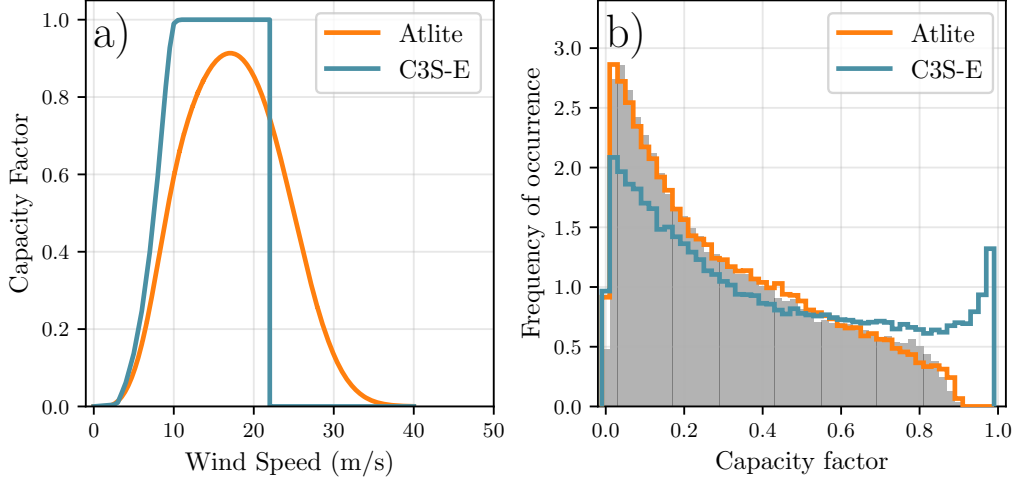


Figure 2: a) Power curves of the Enercon E112.4500 with a 0.3w smoothing filter used by Atlite (orange) and the Vestas V136/3450 used by C3S-E (blue) b) Histograms of wind CF for Ireland from Atlite (orange), C3S-E (blue) and Observed (shaded)

each turbine, as well as losses such as wake effects between turbines, which are important when modelling wind energy on larger spatial scales. The histogram in Fig. 2b shows that the C3S-E power curve tends to underestimate low CF values and overestimate higher ones, whereas the smoothed Atlite power curve more closely follows the observed wind availability data. This is further supported by the percentage of overlap which is higher for Atlite (97.2%) than for C3S-E (83.2%), indicating better agreement with observed data.

The effect of the difference between the power curves is also visible in Fig. 3, which shows a density plot of wind CF values. The two C3S-E datasets are shown to overestimate the observed CF, whereas the Atlite model is in good agreement with the observed data. The skill scores presented in Table 2 show that Atlite performs better than the C3S-E datasets for all of the skill scores.

Fig. 4 shows the average annual number of wind drought events during the 2014 to 2023 validation period. The figure reveals that Atlite presents the best overall agreement with the observed frequency and duration of wind drought events. This pattern is particularly evident for shorter-duration events, which are the most frequent.

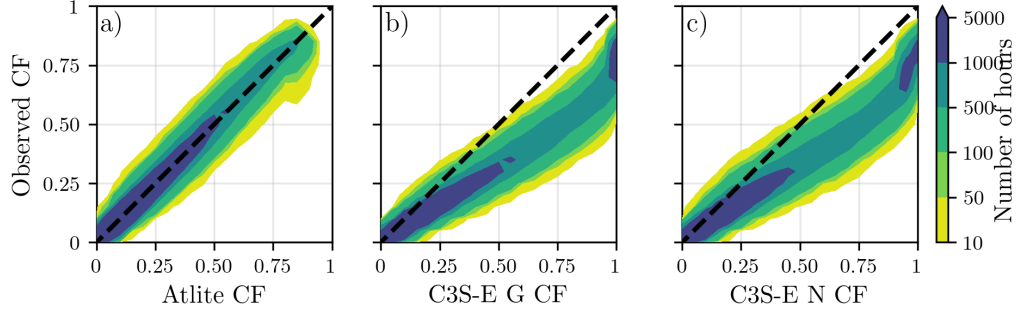


Figure 3: Wind CF density plot of the observed CF (vertical axes) and modelled (horizontal axes) CF data for the a) Atlite, b) C3S-E G and c) C3S-E N datasets

	Atlite	C3S-E G	C3S-E N
CC	0.981	0.972	0.970
RMSE	0.045	0.177	0.162
MBE	-0.003	0.137	0.121

Table 2: Skill scores for wind power for the three datasets compared to observed data

4.1.2. Solar PV Energy

The Atlite model allows the user to select certain PV panel characteristics. In this study, the three PV panel types available in the Atlite model were considered (CSi, CdTe, Kaneka). Following the same methodology as in the previous section, the three available models were compared using four skill scores (CC, RMSE, MBE, and the percentage of overlap). Based on the best-performing metrics, the Beyer PV panel model was selected [26], using the Kaneka Hybrid panel option. For all solar PV farm locations, the azimuth angle is fixed at 180°(due south), and the optimal tilt angle option is applied.

The solar PV installed capacity available on the spreadsheets from EirGrid represents the Maximum Export Capacity (MEC) and does not accurately reflect the installed solar PV capacity. To enable actual solar PV generation potential to be modelled correctly, installed capacities were set at 1.4 times the MEC values. This scaling factor was estimated by analysing proprietary data from individual solar PV farms provided by EirGrid, which showed that, on average, assuming that the installed capacities of farms exceed their MEC values by 40% yields the best agreement with the observed availability.

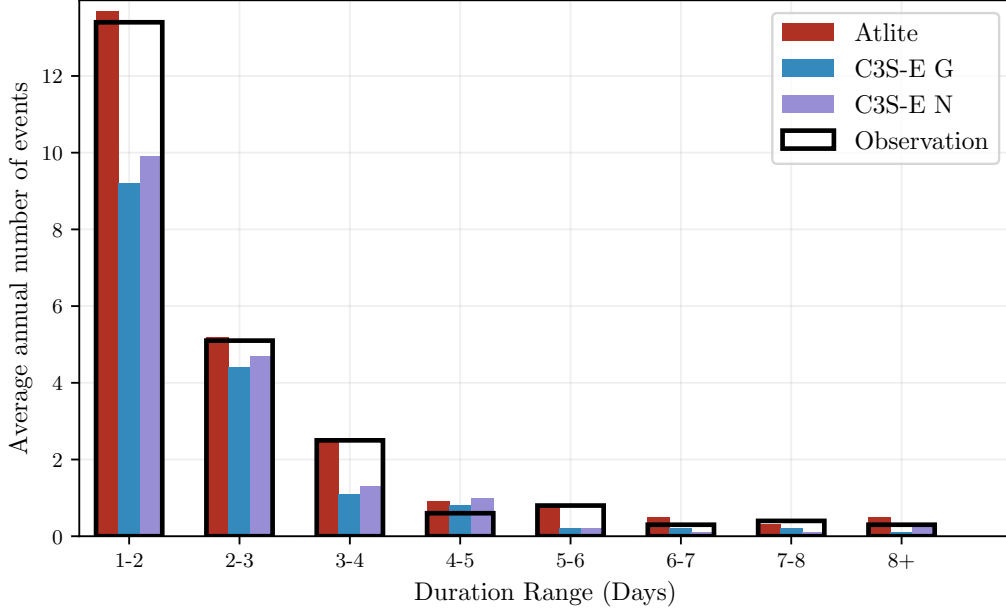


Figure 4: Average annual number of wind drought events for Atlite (red), C3S-E G (blue), C3S-E N (purple), and the observed data (black outline). The wind droughts are identified from 2014 to 2023, considering the actual capacity of the system at any given time

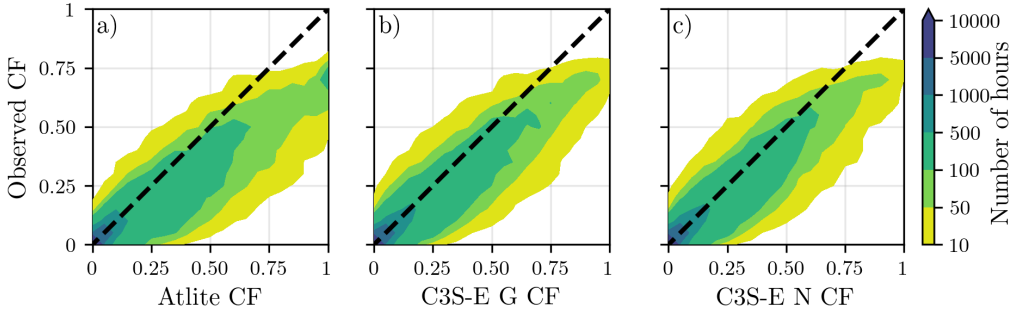


Figure 5: Solar PV CF density plot of the observed (vertical axes) and modelled (horizontal axes) CF series for the a) Atlite, b) C3S-E G and c) C3S-E N datasets

340 Figure 5 shows that the three datasets have a similar tendency to overesti-
 341 mate the CF compared to the observed values, especially for high CF values.
 342 The skill scores presented in Table 3 indicate that C3S-E G performs best
 343 overall, with the lowest RMSE and a high correlation coefficient, suggesting

344 a closer match to observed data. All models show a slight positive bias, with
 345 Atlite exhibiting a slightly lower correlation and higher RMSE.

	Atlite	C3S-E G	C3S-E N
CC	0.921	0.931	0.931
RMSE	0.119	0.090	0.113
MBE	0.046	0.027	0.021

Table 3: Skill scores for Solar PV CF for the three datasets compared to observed data

346 Fig. 6 shows the number of solar PV drought events during the 2023
 347 validation period across different duration ranges. The figure reveals partial
 348 agreement between the three datasets and the observed data, with consistent
 349 results noticed for duration ranges of 1-2, 3-4, 7-8, and 8+ days. However,
 350 discrepancies appear in the other ranges, where the models diverge from the
 351 observed data. The main challenge in validating solar PV data stems from
 352 the recent installation of a large share of Ireland’s solar PV capacity, with
 353 over 65% of the total solar PV capacity installed in 2023. This results in
 354 uncertainties in solar PV generation data and the actual generating capacity
 355 in the first few months after each farm is connected.

356 As the goal of this analysis is to assess the combination of wind and solar
 357 PV generation, the complementary nature of these energy sources mitigates
 358 the limitations in solar PV-only results.

359 4.2. Analysis

360 In this section, RES drought events are evaluated under two different
 361 scenarios with fixed installed capacities: the 91W-9PV scenario, with 5.9
 362 GW of wind capacity and 0.6 GW of solar PV capacity; and the 57W-43PV
 363 scenario, where wind capacity comprises 11.45 GW and solar PV capacity
 364 increases to 8.6 GW. Both scenarios were driven by 45 years of ERA5 data.
 365 Using the RES drought identification process described in Section 3.5, wind
 366 and solar PV droughts are first analysed separately before presenting the
 367 results for combined (wind + solar PV) RES droughts under both scenarios.

368 It is important to highlight that this analysis considers two key aspects:
 369 the absolute values that characterise RES droughts, which are crucial for
 370 power system planning, and the relative differences observed when comparing
 371 the various datasets and energy scenarios described in Section 3.4. This
 372 complete analysis puts forward the differences between the datasets, showing

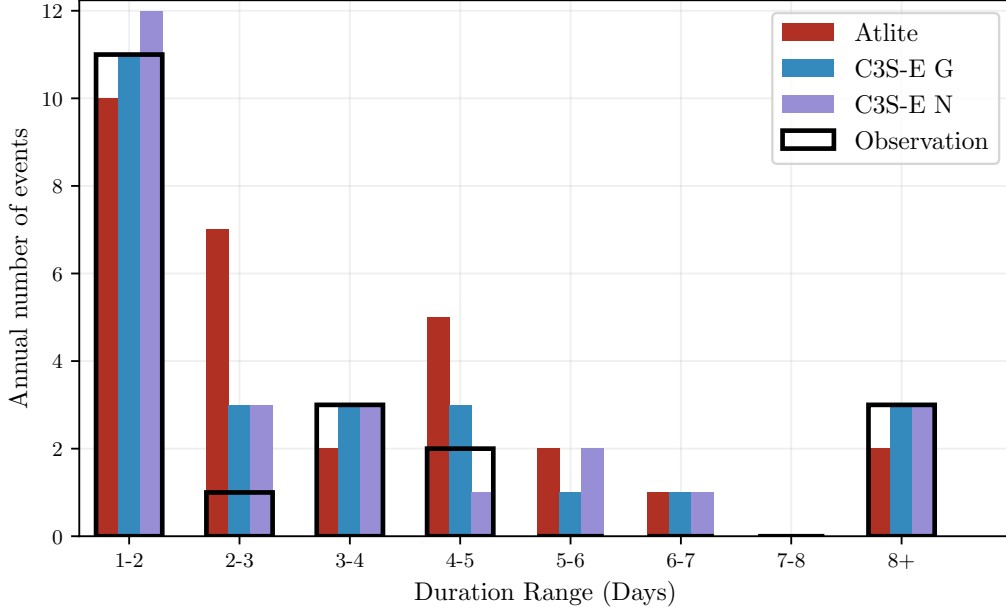


Figure 6: Number of solar PV drought events for Atlite (red), C3S-E G (blue), and C3S-E N (purple) and the observed data (black outline). The solar PV droughts are identified for 2023, considering the actual capacity of the system at any given time

the impact of possible misrepresentations of the system on the analysis of RES drought events.

4.2.1. Annual Number of RES Droughts

The analysis of annual RES drought events reveals trends that are largely consistent with earlier studies. When only wind energy is considered (Fig.7a), the number of drought events decreases as the duration range increases, with very few events lasting more than seven days. This pattern aligns with previous research showing that wind droughts tend to be short and frequent. In contrast, for solar PV energy (Fig.7b), drought frequency declines from one to eight days and then slightly increases for longer durations. This behaviour is attributable to Ireland’s high-latitude location, where reduced sunlight in winter (from November to March) leads to consistently low solar PV output.

Moreover, the comparison between wind and solar PV results indicates that the median, first, and third quartiles for solar PV are consistently higher than or equal to those for wind. This is expected, given that solar PV generation is inherently lower, zero at night, and limited by the solar cycle, as

389 observed in other studies. When wind and solar PV are combined under the
 390 91W-9PV scenario (Fig.7c), the results closely mirror those of wind alone,
 391 reaffirming wind’s dominance in the current energy mix. However, in the
 392 57W-43PV scenario (Fig.7d), a marked reduction in drought events is ob-
 393 served across all datasets, with a decrease of the total number of events of
 394 56% for Atlite, 52% for C3S-E G, and 50% for C3S-E N, demonstrating the
 395 beneficial effects of a more balanced energy mix. These findings are in line
 396 with earlier studies that highlight how increasing solar PV capacity can miti-
 397 gate drought frequency through the anti-correlated seasonal patterns of wind
 398 and solar generation.

399 Additionally, the consistently higher drought counts reported by the Atlite
 400 dataset, compared to the C3S-E datasets, underscore the impact of model
 401 selection, particularly the influence of wind turbine power curve represen-
 402 tation, on quantifying RES droughts. This observation is consistent with
 403 previous research, which has also noted that assumptions regarding turbine
 404 characteristics can significantly affect drought duration estimates.

405 4.2.2. *Return Periods of RES Drought Duration*

406 The RES drought events identified over the 45-year period were used to
 407 calculate the return periods for different RES drought durations. A return
 408 period is the estimated average time interval between events of a specified
 409 duration or intensity (not to be confused with the frequency of their oc-
 410 currence within a fixed time frame). Fig. 8 illustrates the return periods
 411 for varying RES drought durations, highlighting how often different drought
 412 lengths are likely to occur across the datasets. This analysis not only quan-
 413 tifies the likelihood of prolonged low-generation periods but also provides
 414 insight into how extreme events are distributed across different timescales,
 415 helping to assess the variability of rare but impactful events. Understand-
 416 ing these return periods is crucial, as even infrequent droughts can challenge
 417 energy security by placing significant strain on conventional backup sources
 418 necessary to maintain supply in high-RES scenarios.

419 For wind (Fig. 8a), the log-linear increase in return periods observed in
 420 this study confirms that longer droughts occur exponentially less frequently,
 421 a trend consistent with earlier research on wind variability. In the case of so-
 422 lar PV droughts (Fig.8b), the Atlite dataset shows a general log-linear trend,
 423 whereas the C3S-E datasets exhibit a sudden increase in drought duration
 424 for events exceeding sixteen days. This abrupt rise reflects differences in how
 425 solar PV output is handled near the CF threshold during low irradiance con-

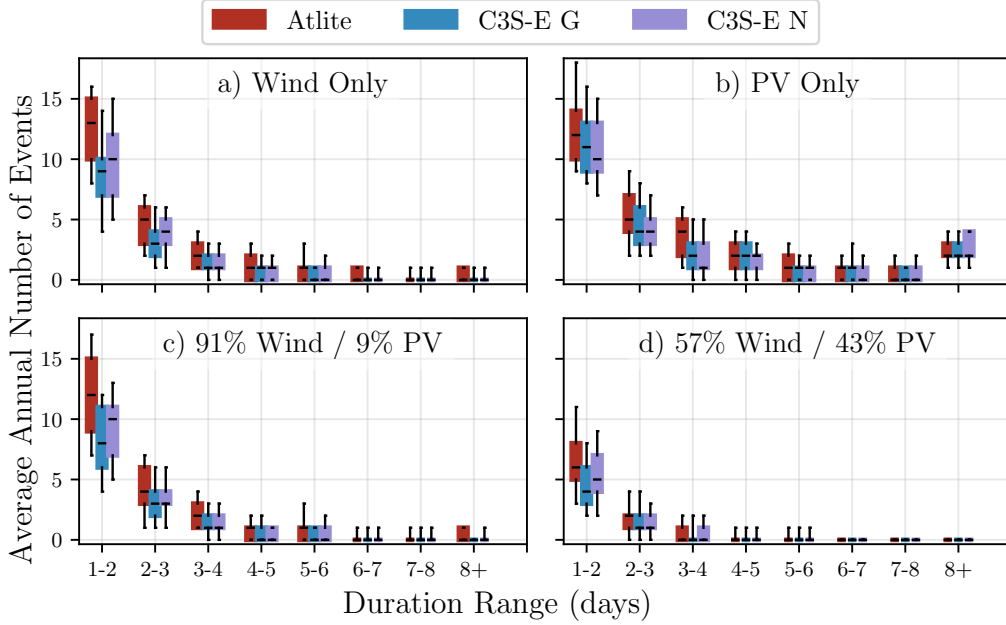


Figure 7: Average annual number of RES droughts (from 1979 to 2023) for a) Wind, b) solar PV, c) 91W-9PV and d) 57W-43PV for Atlite (red), C3S-E G (blue), and C3S-E N (purple). The x-axis represents duration ranges in days (lower bound included), while the y-axis indicates the annual number of events. The boxes display the first and third quartiles and the median is marked by a black line. The whiskers indicate the 5th and 95th percentiles

ditions. In the balanced scenario, the reduced share of wind and increased share of solar PV leverages their complementary seasonal patterns, resulting in higher return periods for combined drought events. This outcome highlights the benefit of a diversified energy mix in enhancing system resilience.

Under the 91W-9PV scenario (Fig. 8c), the combined RES drought return periods largely mirror those for wind alone, reflecting the dominance of wind in the current energy mix. In contrast, the balanced 57W-43PV scenario (Fig. 8d) shows a dramatic increase in return periods across all durations, suggesting that a more diversified energy mix can substantially mitigate the frequency of prolonged drought events.

Across Fig. 8a, c, and, d, the return periods in the Atlite dataset are consistently higher than those in the two C3S-E datasets. For instance, in the 91W-9PV scenario (Fig. 8c), an event with a one-year return period lasts six

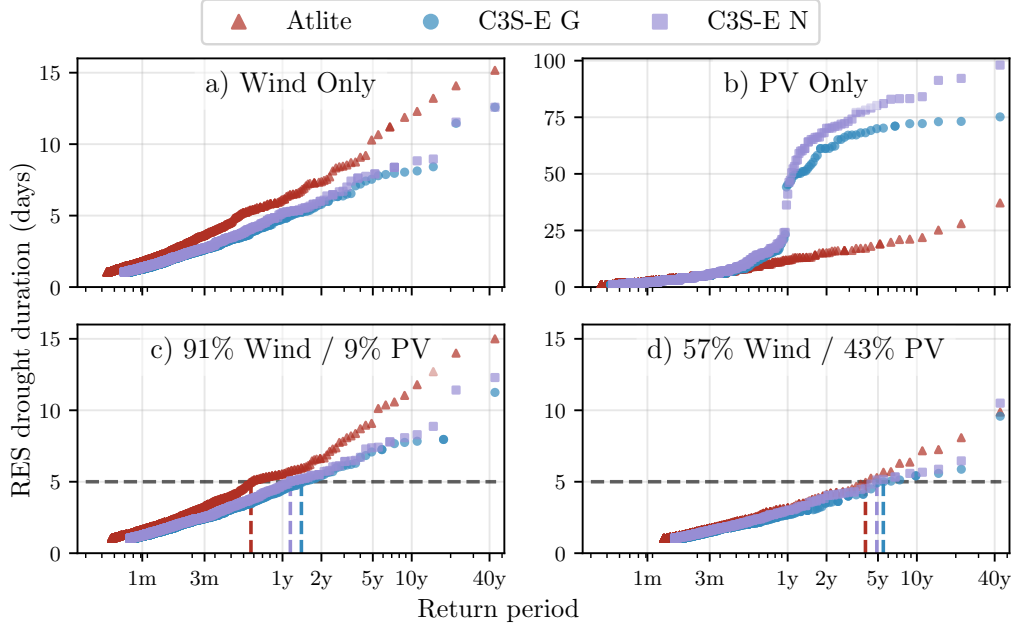


Figure 8: Return periods of the duration of RES droughts (from 1979 to 2023) for a) Wind, b) Solar PV, c) 91W-9PV and d) 57W-43PV for Atlite (red triangle), C3S-E G (blue circle), and C3S-E N (purple square). The x-axis represents the return period time in a log-scale and the y-axis indicates the duration of RES drought associated with it. The horizontal dashed line marks the 5-day return period, with coloured vertical dashed marking its return period for each dataset

439 days in the Atlite dataset, compared to only five days in the C3S-E datasets.
 440 This difference underscores the importance of model selection when quan-
 441 tifying RES droughts, as each dataset’s assumptions and parametrisations
 442 significantly influence drought duration estimates. Additionally, in all four
 443 graphs, the similarity between results from the two C3S-E datasets suggests
 444 that assumptions in the Atlite dataset, such as wind turbine power curve
 445 selection and PV panel specifications, have a greater impact on RES drought
 446 duration estimates than the precise geographic distribution of RES farms
 447 when studying the return periods of RES droughts.

448 4.2.3. Seasonal Distribution of RES Droughts

449 The seasonal analysis of RES droughts is based on the percentage of
 450 hours in each month classified as drought events. Wind droughts tend to
 451 be more frequent during summer, whereas solar PV droughts are more com-

mon in winter due to reduced sunlight. By comparing these seasonal patterns across different datasets and energy scenarios, the study examines how model-specific assumptions and variations in capacity mix affect the overall characterisation of drought events.

For the wind-only scenario (Fig. 9a), the Atlite dataset exhibits a pronounced seasonal pattern, with about 24% of summer hours (June–July–August) identified as droughts compared to only 4% in winter (December–January–February). This strong seasonal signal is less evident in the C3S-E datasets, which suggests that the differences in the underlying wind power curves play a significant role. In Atlite, CF near or below the 0.1 threshold occurs at relatively higher wind speeds, resulting in a higher count of drought hours during the summer months. In contrast, solar PV droughts (Fig. 9b) display an opposite seasonal trend. Across all datasets, over 60% of winter hours are classified as solar PV droughts, reflecting the naturally low solar irradiance in Ireland during winter. Moreover, Atlite tends to record a slightly higher percentage of drought hours for wind and a marginally lower percentage for solar PV relative to the C3S-E datasets. These differences highlight how dataset-specific assumptions, such as the treatment of wind turbine power curves and PV panel characteristics, significantly influences the apparent seasonal dynamics of RES droughts.

The 91W-9PV scenario (Fig. 9c) shows patterns comparable to the ones for wind droughts (Fig. 9a). However, in the 91W/9PV scenario, the number of hours classified as RES droughts in summer decreases slightly compared to the wind-only scenario. This reduction can be explained by the contribution of solar PV generation during the summer months in the 91W-9PV scenario, even though it constitutes only 11% of total capacity. Since the number of RES drought hours for solar PV in summer is near zero, this small contribution has a noticeable impact on reducing overall drought hours. In the 57W-43PV scenario (Fig. 9d), all three datasets show a reduction in monthly RES drought frequency. Annual reductions in median RES drought frequency are observed across the datasets, dropping from 14% to 5% for Atlite, from 8% to 3% for C3S-E G, and from 9% to 4% for C3S-E N. The balanced mix of wind and solar PV power in this scenario reduces the seasonal signal overall and significantly decreases the percentage of RES drought hours in the summer.

The seasonal variations observed in this study have important implications for energy planning. Given that energy demand peaks in winter for Northern European countries, understanding these seasonal patterns is critical for assessing the need for conventional backup or storage solutions during

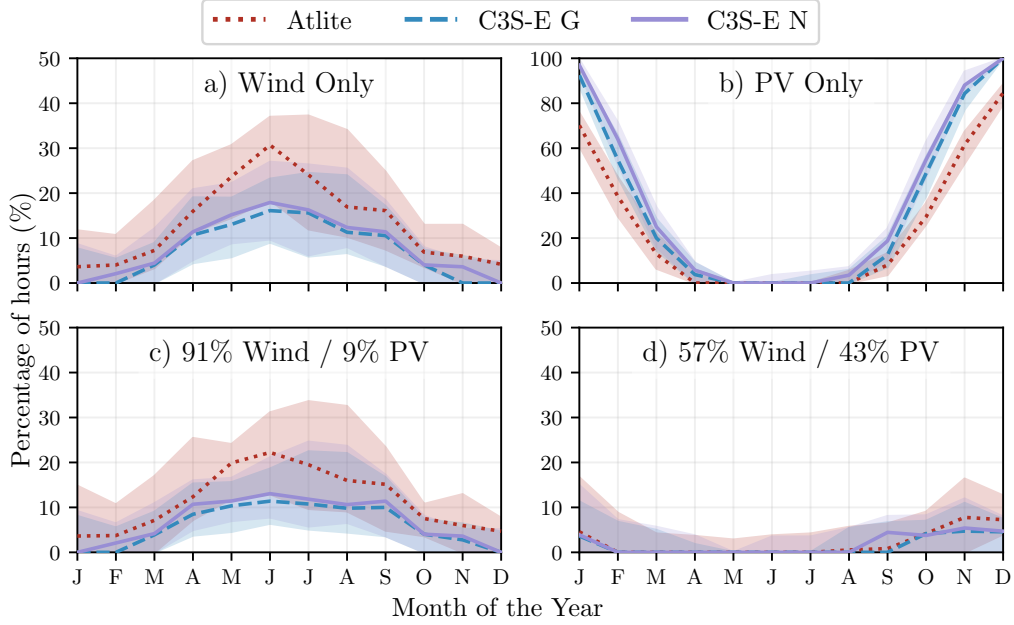


Figure 9: Percentage of hours in a month which are part of a RES drought (from 1979 to 2023) for a) Wind, b) Solar PV, c) 91W-9PV and d) 57W-43PV for Atlite (red dotted), C3S-E G (blue dashed), and C3S-E N (purple solid). The x-axis represents the month of the year, and the y-axis indicates the percentage of hours. Lines correspond to the median values and the area between the first and third quartiles is shaded. Note the different y-axis scale for b).

490 periods of prolonged low renewable output. The findings underscore that
 491 even small differences in model assumptions leads to significant variations in
 492 drought estimates, thereby affecting the reliability of the energy system dur-
 493 ing critical periods. Such insights are essential for policymakers to develop
 494 targeted strategies that enhance grid resilience and ensure a stable energy
 495 supply throughout the year.

496 5. Conclusions

497 This study has investigated the ability of three RES datasets to repre-
 498 sent RES droughts: Atlite, C3S-E G, and C3S-E N. One of the most evident
 499 differences is how each dataset incorporates the specific locations of RES
 500 farms. Both Atlite and C3S-E G consider the locations of wind and solar PV
 501 farms, which one would expect to result in a more accurate representation

502 of RES generation. While this approach slightly improves solar PV mod-
503 els, our analysis indicates that for wind energy, the Atlite dataset performs
504 better overall, especially in its close alignment with observed data for wind
505 generation estimates. This finding suggests that, although the inclusion of
506 RES farm locations is beneficial, the accuracy of the RES dataset is more
507 strongly influenced by underlying model assumptions, such as selecting an
508 appropriate wind power curve.

509 Atlite shows the best alignment with observed data for wind generation.
510 Differences between the datasets are smaller for solar PV, with C3S-G per-
511 forming marginally better than the other two. The results show that the
512 two C3S-E datasets (C3S-E G and C3S-E N) consistently yield similar out-
513 comes, indicating that their methodological differences have minimal impact
514 in this case. This distinction is also evident in the analysis, where Atlite
515 reports higher return periods and a greater number of RES droughts, espe-
516 cially in scenarios with a balanced share of RES. Again, the results from RES
517 drought modelling rely more on the precision of the wind power curve and
518 PV panel models than on the specific locations of RES farms. Atlite's supe-
519 rior performance highlights the importance of selecting validated models for
520 assessing RES drought risks. This careful model selection can better quantify
521 risks, support effective planning, and avoid the potential underestimation of
522 capacity needs, which is essential for ensuring energy security.

523 Looking at the 57W-43PV scenario, the analysis showed a significant im-
524 provement in the management of RES droughts due to the complementary
525 nature of wind and solar PV generation. Wind and solar PV together perform
526 better in terms of reducing drought frequency and duration than either would
527 individually, largely because of the seasonal anti-correlation between the two
528 energy sources. This diversification reduces the seasonal impact on RES
529 droughts, as solar PV generation peaks in the summer and wind generation
530 is more consistent in winter. Ireland currently has a highly wind-dependent
531 energy system, but with ambitious targets for solar PV installations in the
532 coming years, the energy mix is expected to approach a balance between wind
533 and solar PV capacity. While this balanced approach offers a more stable
534 and secure energy supply by mitigating RES drought risks, it is important
535 to note that having similar wind and solar PV capacities may not optimise
536 other aspects, such as annual energy production or meeting nighttime loads.
537 For policymakers, these findings underscore the importance of meeting these
538 capacity targets to enhance energy security through diversification. Addition-
539 ally, the choice of model for RES drought assessment becomes increasingly

critical as more renewable capacity is integrated into the system.

This study has several limitations. Although ERA5 is among the best reanalysis datasets for renewable energy analysis, its resolution may not capture local-scale phenomena, making it less reliable at the individual farm level. In addition, previous studies have indicated biases in ERA5 variables especially wind speed. Moreover, the methodology employs a fixed threshold to define RES drought events, which is necessary for comparing the three models but does not account for demand variations. Consequently, while this approach enables a consistent inter-comparison, it may overlook events that are most critical for power system operations.

Future work is planned to extend the current analysis. First, climate projection data will be integrated with different energy scenarios, incorporating the addition of offshore wind, to better understand how climate change might affect RES droughts. Second, expanding the geographic domain of the study to include the rest of Europe would provide a more comprehensive understanding of RES droughts in an interconnected energy grid. This would require extensive verification across other European countries, making it a more complex but highly relevant challenge.

Data Availability

The ERA5 data can be obtained from the Climate Data Store (<https://doi.org/10.24381/cds.adbb2d47>). The C3S-E dataset is also available from the Climate Data Store (<https://doi.org/10.24381/cds.4bd77450>). Information on wind and solar PV farms in Ireland can be obtained from the EirGrid website (<https://www.eirgrid.ie/grid/system-and-renewable-data-reports>). The Atlite model used in this study is open-source and can be found on GitHub (<https://github.com/pypsa/atlite>). The data and code required to reproduce the analysis in this article will be made available upon acceptance of the manuscript in a public GitHub repository.

Acknowledgments

The research conducted in this publication was funded by Science Foundation Ireland and co-funding partners under grant number 21/SPP/3756 through the NexSys Strategic Partnership Programme.

References

- [1] EuroStat, Renewable Energy Statistics, 2023. URL: https://ec.europa.eu/eurostat/statistics-explained/index.php?title=Renewable_energy_statistics, Accessed: 2024-11-06.
- [2] H. C. Bloomfield, D. J. Brayshaw, L. C. Shaffrey, P. J. Coker, H. E. Thornton, Quantifying the increasing sensitivity of power systems to climate variability, *Environmental Research Letters* 11 (2016) 124025. doi:10.1088/1748-9326/11/12/124025.
- [3] H. C. Bloomfield, D. J. Brayshaw, A. Troccoli, C. M. Goodess, M. De Felice, L. Dubus, P. E. Bett, Y.-M. Saint-Drenan, Quantifying the sensitivity of european power systems to energy scenarios and climate change projections, *Renewable Energy* 164 (2021) 1062–1075. doi:10.1016/j.renene.2020.09.125.
- [4] F. Kaspar, M. Borsche, U. Pfeifroth, J. Trentmann, J. Drücke, P. Becker, A climatological assessment of balancing effects and shortfall risks of photovoltaics and wind energy in germany and europe, *Advances in Science and Research* 16 (2019) 119–128. doi:10.5194/asr-16-119-2019.
- [5] F. Mockert, C. M. Grams, T. Brown, F. Neumann, Meteorological conditions during periods of low wind speed and insolation in Germany: The role of weather regimes, *Meteorological Applications* 30 (2023) e2141. doi:10.1002/met.2141.
- [6] M. Ohba, Y. Kanno, D. Nohara, Climatology of dark doldrums in japan, *Renewable and Sustainable Energy Reviews* 155 (2022) 111927. doi:10.1016/j.rser.2021.111927.
- [7] M. J. Mayer, B. Biró, B. Szűcs, A. Aszódi, Probabilistic modeling of future electricity systems with high renewable energy penetration using machine learning, *Applied Energy* 336 (2023) 120801. doi:10.1016/j.apenergy.2023.120801.
- [8] D. Raynaud, B. Hingray, B. François, J. Creutin, Energy droughts from variable renewable energy sources in European climates, *Renewable Energy* 125 (2018) 578–589. doi:<https://doi.org/10.1016/j.renene.2018.02.130>.

- [9] A. Gangopadhyay, A. K. Seshadri, N. J. Sparks, R. Toumi, The role of wind-solar hybrid plants in mitigating renewable energy-droughts, *Renewable Energy* 194 (2022) 926–937. doi:10.1016/j.renene.2022.05.122.
- [10] J. Kapica, J. Jurasz, F. A. Canales, H. Bloomfield, M. Guezgouz, M. De Felice, Z. Kobus, The potential impact of climate change on european renewable energy droughts, *Renewable and Sustainable Energy Reviews* 189 (2024) 114011. doi:10.1016/j.rser.2023.114011.
- [11] K. Z. Rinaldi, J. A. Dowling, T. H. Ruggles, K. Caldeira, N. S. Lewis, Wind and Solar Resource Droughts in California Highlight the Benefits of Long-Term Storage and Integration with the Western Interconnect, *Environmental Science and Technology* 55 (2021) 6214–6226. doi:10.1021/acs.est.0c07848.
- [12] P. T. Brown, D. J. Farnham, K. Caldeira, Meteorology and climatology of historical weekly wind and solar power resource droughts over western North America in ERA5, *SN Applied Sciences* 3 (2021) 814. doi:10.1007/s42452-021-04794-z.
- [13] S. Allen, N. Otero, Standardised indices to monitor energy droughts, *Renewable Energy* 217 (2023) 119206. doi:10.1016/j.renene.2023.119206.
- [14] C. Bracken, N. Voisin, C. D. Burleyson, A. M. Campbell, Z. J. Hou, D. Broman, Standardized benchmark of historical compound wind and solar energy droughts across the Continental United States, *Renewable Energy* 220 (2024) 119550. doi:https://doi.org/10.1016/j.renene.2023.119550.
- [15] H. Lei, P. Liu, Q. Cheng, H. Xu, W. Liu, Y. Zheng, X. Chen, Y. Zhou, Frequency, duration, severity of energy drought and its propagation in hydro-wind-photovoltaic complementary systems, *Renewable Energy* (2024) 120845. doi:10.1016/j.renene.2024.120845, 2.
- [16] H. Hersbach, B. Bell, P. Berrisford, S. Hirahara, A. Horányi, J. Muñoz-Sabater, J. Nicolas, C. Peubey, R. Radu, D. Schepers, et al., The ERA5 global reanalysis, *Quarterly Journal of the Royal Meteorological Society* 146 (2020) 1999–2049. doi:10.1002/qj.3803.

- [17] L. Dubus, Y. Saint-Drenan, A. Troccoli, M. De Felice, Y. Moreau, L. Ho-Tran, C. Goodess, R. Amaro E Silva, L. Sanger, C3S Energy: A climate service for the provision of power supply and demand indicators for Europe based on the ERA5 reanalysis and ENTSO-E data, *Meteorological Applications* 30 (2023) e2145. doi:10.1002/met.2145.
- [18] F. Hofmann, J. Hampp, F. Neumann, T. Brown, J. Hörsch, Atlite: a lightweight Python package for calculating renewable power potentials and time series, *Journal of Open Source Software* 6 (2021) 3294. doi:10.21105/joss.03294.
- [19] A. Kies, B. U. Schyska, M. Bilousova, O. El Sayed, J. Jurasz, H. Stoecker, Critical review of renewable generation datasets and their implications for european power system models, *Renewable and Sustainable Energy Reviews* 152 (2021) 111614. doi:10.1016/j.rser.2021.111614.
- [20] EirGrid & SONI, System and Renewable Data Reports, 2023. URL: <https://www.eirgrid.ie/grid/system-and-renewable-data-reports>, Accessed: 2024-11-06.
- [21] E. Doddy Clarke, S. Griffin, F. McDermott, J. Monteiro Correia, C. Sweeney, Which reanalysis dataset should we use for renewable energy analysis in ireland?, *Atmosphere* 12 (2021) 624. doi:10.3390/atmos12050624.
- [22] Y.-M. Saint-Drenan, L. Wald, T. Ranchin, L. Dubus, A. Troccoli, An approach for the estimation of the aggregated photovoltaic power generated in several European countries from meteorological data, *Advances in Science and Research* 15 (2018) 51–62. doi:10.5194/asr-15-51-2018.
- [23] I. Staffell, S. Pfenninger, Using bias-corrected reanalysis to simulate current and future wind power output, *Energy* 114 (2016) 1224–1239. doi:10.1016/j.energy.2016.08.068.
- [24] Government of Ireland, Climate Action Plan 2024, Technical Report 3, Department of the Environment, Climate and Communications, 2023. URL: <https://www.gov.ie/pdf/?file=https://assets.gov.ie/>

- 670 284675/70922dc5-1480-4c2e-830e-295afd0b5356.pdf, Accessed:
671 2024-11-06.
- 672 [25] Sustainable Energy Authority Ireland, National Energy Projections
673 2024, Technical Report, Sustainability Energy Authority of Ireland,
674 2024. URL: <https://www.seai.ie/news-and-events/news/energy-projections-report>, Accessed: 2024-11-06.
675
- 676 [26] H. G. Beyer, G. Heilscher, S. Bofinger, A robust model for the mpp
677 performance of different types of pv-modules applied for the performance
678 check of grid connected systems, Eurosun (2004) 8.